TOWARDS THE ASSESSMENT OF LOW-VELOCITY IMPACT INDUCED DAMAGE IN LAMINATE COMPOSITE PLATES

É. Trousset[1*], J. Rannou[1], F. Laurin[1], L. Guillaumat[2], J.-F. Maire[1]

[1]*Onera – The French Aerospace Lab, BP 72 – 29 avenue de la Division Leclerc, FR-92322 CHATILLON cedex*
[2]*Arts et Métiers ParisTech Angers, 2 boulevard du Ronceray - BP 3525, 49035 ANGERS cedex 1, France*
**emilie.trousset@onera.fr*

Keywords: Composites, low-velocity impact, damage, finite element analysis.

Abstract
The sensitivity of composite structures to small shocks is a major issue. Nowadays, this sensitivity is evaluated through cost effective experimental campaigns. A way to reduce testing is to resort to numerical evaluation of impact damage creation, then to use this damage prediction to evaluate the loss of performance of the composite structure. This paper presents an impact modelling using recent developments of the Onera Progressive Failure Models for the unidirectional ply behaviour and cohesive zone models to study delamination. Impact and indent tests have been performed to compare the numerical results to the experimental ones. The first results are encouraging and improvements to apply to the unidirectional ply behaviour law have been identified.

1 Introduction
Some critical parts of aircrafts are now made of composite materials, thanks to their high specific properties. However, these materials are particularly sensitive to low-velocity impacts. For example, a dropped tool during a maintenance operation or a shock during manufacture can create internal damage that might not be detected. Therefore, the possible damage caused by an impact must be taken into account to design composite structures. Nowadays, the impact properties of composite materials are estimated through heavy experimental campaigns, repeated every time the material is changed. Those campaigns have helped to understand the main damage mechanisms due to impacts on composite materials [1-3]. But the costs of those campaigns definitely need to be lightened: hence the necessity of numerical simulations.
For several years, Onera has developed advanced behaviour models for composite materials, mainly for quasi-static and in-plane loading [4]. Our goal is to determine if we can extend these models to dynamic and out-of-plane cases, like low-velocity impact events, and to evaluate their ability to predict the damage states in such conditions.
The ply behaviour law and possibly cohesive zone models, that can describe both initiation and propagation of delamination, are applied to a numerical model built to reproduce a special drop-weight impact test. Impact and quasi-static tests are performed for further comparisons with the computational results.

2 Material models

2.1 Unidirectional ply behaviour, damage and failure

The Onera Progressive Failure models (OPFM) [4] describe the unidirectional ply behaviour and predict the final failure of laminated specimens. The model coefficients are identified by simple tests and this approach enables the prediction of the initiation and propagation of damage in laminates. When the first cracks are detected, the unidirectional ply properties are degraded to describe the damaged behaviour of the ply. Then, when a catastrophic failure mode is reached (such as fibre failure or matrix failure in compression), the behaviour of the laminate is described by a softening law.

2.1.1 Behaviour of the ply

In order to accurately predict damage and failure in laminates, it is necessary to describe the behaviour in a correct manner (correct estimation of stresses and strains) prior to the first cracks. First, the unidirectional ply is assumed to be transversely isotropic. The initial law is non linear thermo-viscoelastic (1).

$$\sigma = \tilde{C}\left(\varepsilon - \varepsilon_{ve} - \varepsilon_{th} - \varepsilon_{nl}\right) \tag{1}$$

The longitudinal elasticity (ε_{nl}) is non linear, to describe the reinforcement in tension and the softening in compression experimentally observed in the fibre direction [5]. The manufacturing process of laminates (autoclave curing) induces thermal residual stresses in plies that have a significant role on the onset of transverse crack. In the OPFM, they are classically introduced through a thermal strain, ε_{th}. The viscoelasticity of the thermoset polymer matrix is taken into account to model the non linear response of the unidirectional ply under shear loading but also the strain rate effects. The viscoelasticity is introduced in the model as a viscoelastic strain, ε_{ve} (2).

$$\varepsilon = \varepsilon_e + \varepsilon_{ve} \quad with \quad \dot{\varepsilon}_{ve} = g(\sigma)\sum_{i=1}^{N}\dot{\xi}_i \tag{2}$$

The main idea of the non linear viscoelastic approach is to assume that the viscosity can be decomposed into elementary viscous mechanisms (ξ_i), defined by their relaxation times and weights. Moreover, $g(\sigma)$ is a non linearising function taking into account the non linearity of the organic matrix composite viscoelasticity, essential to accurately describe creep tests with different stress levels.

2.1.2 Failure criteria

There are two criteria for each failure mode (longitudinal and in-plane interfibre) and the mechanisms involved in tension and compression are separately considered. These criteria are summed up in table 1.

In the longitudinal direction, the coupling is made between the in-plane matrix damage state d_2 and the tensile longitudinal strength. In-plane and out-of-plane shear effects on longitudinal compression strengths are taken into account.

In the transverse direction, the effect of early fibre failure is taken into account in the transverse criteria threshold (through the variable d_{12}^f). The coupling between the transverse compression and the in-plane and out-of-plane shear loadings is made. The p_{ij} parameters represent the reinforcement of the apparent mesoscopic strengths for high shear and low transverse compression loadings and the weakening for shear and transverse tension.

Fibre failure	Tensile failure ($\sigma_{11}\geq 0$)	$f_1^+ = \left(\frac{\sigma_{11}}{X_t^{UD} e^{-h_{2r} d_2} + X_t^{dry}\left(1 - e^{-h_{2r} d_2}\right)} \right)^2 = 1$
	Compressive failure ($\sigma_{11}<0$)	$f_1^- = \left(\frac{\sigma_{11}}{X_c} \right)^2 + \left(\frac{\tau_{12}}{S_{12}^f (1 - p_{12}\sigma_{22})} \right)^2 + \left(\frac{\tau_{23}}{S_{13}^f (1 - p_{13}\sigma_{33})} \right)^2 = 1$ *with* $S_{12}^f = \frac{S_{12}^R}{\sqrt{1 - f_{6\to 1}^2}}$ *and* $S_{13}^f = \frac{S_{13}^R}{\sqrt{1 - f_{5\to 1}^2}}$
In-plane interfibre failure	Tensile failure ($\sigma_{22}\geq 0$)	$f_2^+ = \left(\frac{\sigma_{22}}{Y_t} \right)^2 + \left(\frac{\tau_{12}}{S_{12}^R (1 - p_{12}\sigma_{22})} \right)^2 + \left(\frac{\tau_{23}}{S_{23}^R (1 - p_{23}\sigma_{33})} \right)^2 = \left(1 - d_{12f}\right)^2$
	Compressive failure ($\sigma_{22}<0$)	$f_2^- = \left(\frac{\sigma_{22}}{Y_c} \right)^2 + \left(\frac{\tau_{12}}{S_{12}^R (1 - p_{12}\sigma_{22})} \right)^2 + \left(\frac{\tau_{23}}{S_{23}^R (1 - p_{23}\sigma_{33})} \right)^2 = \left(1 - d_{12f}\right)^2$
X_t^{UD}, X_t^{dry}, Y_t: Tensile longitudinal and transverse strengths X_c, Y_c: Compressive longitudinal and transverse strengths S_{12}^R, S_{13}^R, S_{23}^R: Plane and out-of-plane shear strengths S_{12}^f, S_{13}^f: in-plane and out-of-plane shear strength in fibre mode $f_{6\to 1}$, $f_{5\to 1}$: shape parameters		

Table 1. Failure criteria of the OPFM for the unidirectional ply [6]

2.1.3 Damage behaviour

The damage modelling is done in the thermodynamic framework of irreversible processes. Each failure mechanism leads to a deterioration of the laminate elastic properties (3).

$$\tilde{S} = S^0 + d_1 H_1 + d_2 H_2 \quad with \quad \tilde{C} = \tilde{S}^{-1} \tag{3}$$

H_1 and H_2 are the effect tensors associated to each damage variable, respectively d_1 for fibre failure and d_2 for in-plane interfibre failure. These scalar variables represent the progressive deterioration kinetics of the damaged ply. The degradation kinetics describes the evolution of the effective rigidity of the ply, in the laminate, across the loading (4-5).

$$d_1 = \alpha \left\langle \sqrt{f_1} - 1 \right\rangle^+ \quad with \quad f_1 = \eta_1 f_1^+ + (1 - \eta_1) f_1^-, \quad \eta_1 = \begin{cases} 0 \; if \; \sigma_{11} \geq 0 \\ 0 \; if \; \sigma_{11} < 0 \end{cases} \quad and \quad \dot{d}_1 \geq 0 \tag{4}$$

$$d_2 = \beta \left\langle \sqrt{f_2} - 1 \right\rangle^+ \quad with \quad f_2 = \eta_2 f_2^+ + (1 - \eta_2) f_2^-, \quad \eta_2 = \begin{cases} 0 \; if \; \sigma_{22} \geq 0 \\ 0 \; if \; \sigma_{22} < 0 \end{cases} \quad and \quad \dot{d}_2 \geq 0 \tag{5}$$

The unilateral aspect of damage is taken into account. The unidirectional behaviour law has been implemented into the finite element code *Z-set*, developed by Onera, Mines ParisTech and Northwest Numerics & Modelling Inc. Links exist to use it in other finite element codes, like *Abaqus* or *Samcef*.

2.2 Cohesive zone models

A major damage mode in composite laminates is delamination. In the previous model, the effect of delamination is represented by the d_3 scalar damage variable, in the ply. But other methods exist to model delamination between two plies of different orientations. Among the different modelling techniques for delamination, cohesive zone models can describe both initiation and propagation of delamination. As these two aspects of delamination occur during an impact event, cohesive zone models have been chosen in this study.

A cohesive zone element is a surface element, whose nodes are split in half. A cohesive law is associated to the element, so that its nodes can move one from another, according to the

loading. When the damage variable associated to the law reaches its maximum, the element is considered as broken. The breakage can occur in opening or sliding modes.
The normal (U_n) and tangential displacements of the element nodes are functions of the normal (T_n) and tangential forces applied to them (Figure 1). In this study, the Crisfield cohesive law [8] has been chosen. The initial slope is chosen as high as possible, as the interface is initially supposed infinitely rigid. When the stress threshold (T_n max) is reached, the element is softly deteriorated. The damage variable (λ) is set (6), going from 0 to 1, where the element is considered as broken.

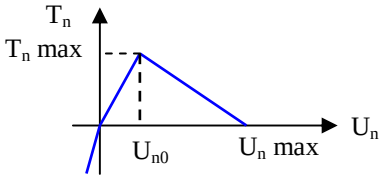

Figure 1. Crisfield behaviour law [8], represented for the opening mode

$$\lambda = \frac{1}{\eta}\frac{\langle\kappa\rangle}{1+\langle\kappa\rangle}, \quad \kappa = \sqrt{\left(\frac{\langle U_n\rangle}{U_{n0}}\right)^2 + \left(\frac{\|\vec{U}_t\|}{U_{t0}}\right)^2}, \quad \eta = 1 - \frac{U_{n0}}{U_{n_{max}}} = 1 - \frac{U_{t0}}{U_{t_{max}}} \tag{6}$$

The main issue with the use of cohesive zone elements is the necessity to have a fine mesh, in order to accurately capture the delamination initiation. It is also important to detect solution jumps, especially in static resolution cases. Once the models are identified by simple tests (DCB, ENF), the purpose is to study their validity on low-velocity impact cases.

3 Numerical models

The numerical model of the composite laminate plate represents the free part of a 100x100 mm² plate embedded between two steal plates with 70 mm diameter holes in the middle (Figure 2a). The target mesh is a 70 mm diameter circular plate, with a 4.16 mm thickness. This thickness corresponds to the one of a 16-ply laminate. The chosen element type is the linear full integrated prismatic element (C3D6 - Figure 2b). The volume elements are required for the use of the previous ply law. There is one element by ply through the thickness. In order to limit the size of the numerical problem, the mesh size is refined in the potential zone of delamination initiation, and then the mesh size linearly grows to reach the maximum fixed mesh size. In order to avoid perturbation by the stress gradient due to the embedding of the plate in the impact stress gradient, the mesh is refined near the bounds of the numerical model of the plate. The value of the displacements of the circumference of the upper and lower surfaces of the plate is maintained to zero (Figure 2c).

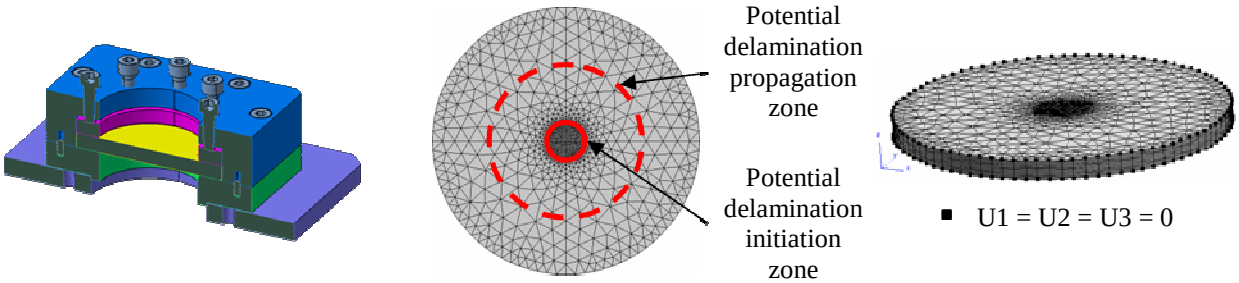

Figure 2. Cut of the embedding device (a), *Z-set* plate mesh (b) and boundary conditions (c)

The 16 mm diameter hemispherical modelled impactor is the one described in the ASTM standard for impact tests [9]. The impactor is meshed with linear full integrated continuum 3D elements with 4 nodes.

4 Experimental data

Drop-weight impact and indentation tests have been performed on embedded $[(45°/90°/-45°/0°)_2]_s$ quasi-isotropic laminates made of T700GC carbon fiber and M21 epoxy matrix with a weight area of 268 g/m^3.

4.1 Impact testing

Drop-weight impact tests were performed on a Dynatup 8250 of GRC Instruments apparatus. The original clamping device of the target was replaced by the embedding assembly shown on a, in order to have a better confidence into the boundary conditions imposed on the numerical plate mesh. The impactor is a 16 mm diameter hemisphere and weighs 6.36 kg [9]. Five impact energies were chosen: 5, 10, 18, 20 and 28 Joules. During the tests, the force history was measured with a force cell and the displacements of the point opposite to impact history were measured with a laser. After the impact tests, the residual impact depth was measured by digital image correlation (Figure 3a) and ultrasonic scans allowed to see the damage created by the impact (Figure 3b). The damage depth maps were used to estimate the projected damage area. Specimens impacted at 20 Joules presented a reasonable damage size for further microscopic observation. Those specimens were then cut to observe the different damages in the plates (transverse cracks and delamination - Figure 3c).

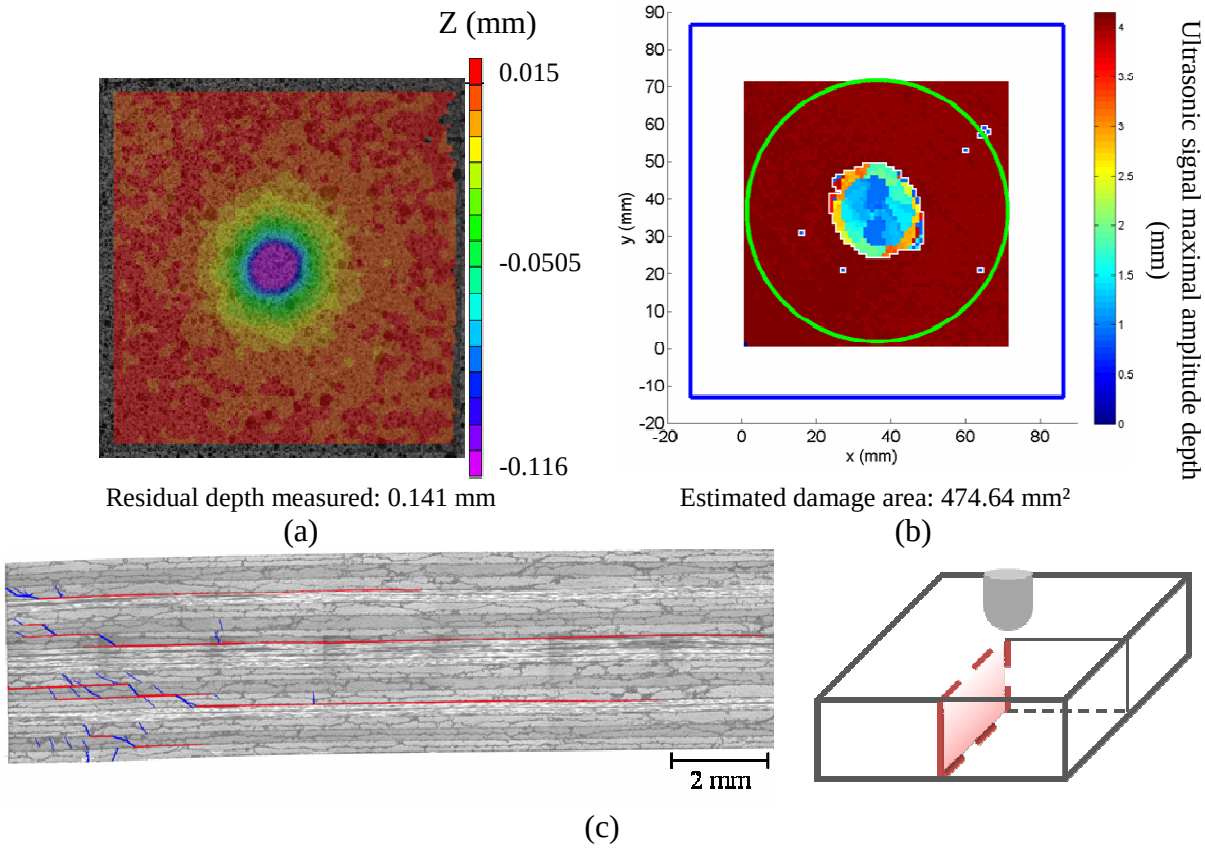

Figure 3. Residual depth (a) and damage through the thickness depth (b) of a quasi-isotropic laminate impacted at 10 J and micrograph the damaged zone of a quasi-isotropic laminate impacted at 20 J (c). The intralaminar cracks are colored in blue and the delamination is colored in red.

A classic impact pattern of failure is observed on figure 3c, which is a pine tree shape of damage through the thickness. The upper transverse cracks of the cut edge are inclined at around 53° and are due to out-of-plane stresses. They are getting vertical, through the thickness. The lower cracks are vertical due to in-plane transverse stresses and in-plane shear.

4.2 Quasi-static testing

The maximal impact forces measured during the impact tests were used to lead the quasi-static tests. The displacement velocity of the punch was constant (0.6 mm/min). Once the demanded maximal force was reached, the punch was brought back up at the same velocity. During the test, the force history was measured with a force cell and the displacements of the point opposite to the indent point were measured with a linear variable differential transformer. The slowness of the indentation test allowed the use of acoustic emission during the test, to monitor the damage evolution. Some tests had strain gauges on the non indented face for further comparisons with numerical results. After the tests, the residual indent depth and the damage created were measured and observed in the same way as for impact tests. The indented specimens, corresponding to 20J impacts, were cut for microscopic observations of the damage (Figure 4).

The damage created by indentation seems quite identical to the one obtained by impact. The delaminated interfaces are the same. Indent testing has a better repeatability than impact testing. Moreover, the instrumentation of the indent test is richer, so that more information is extracted from this type of tests. This is why indentation tests are important to understand the damage mechanisms that occur during an impact event.

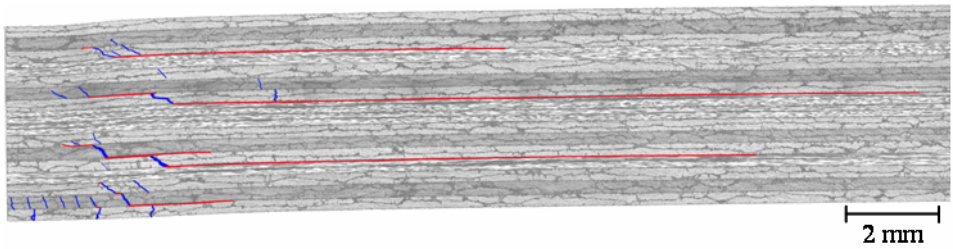

Figure 4. Micrograph of the damaged zone of a quasi-isotropic laminate indented at 10 kN, equivalent to the maximum force measured for the 20 J impact test. The intralaminar cracks are colored in blue and the delamination is colored in red.

5 Computational and experimental results confrontation

The finite element code *Z-set* is used for a dynamic implicit resolution (Newton-Raphson). In *Z-set*, the chosen contact management is the flexibility method [10]. This method is not intrusive but, for impact problems, leads to high computation costs. 90 % of the computation time is dedicated to the contact solve, which is too high. Improvements have been recently done and are currently being implemented. In order to get rid of contact in *Z-set*, a strategy may consist in running a linear elastic impact problem, to extract the effective contact nodes displacements along the out-of-plane direction and to impose them on the same nodes of the plate mesh instead of the contact resolution. Studies could then be performed with richer behaviour laws, in a more acceptable time. Comparison between computational and experimental results is done on a 10 J impact case. The numerical resolution is made through implicit dynamics and the contact problem is replaced by the displacements calculated on the nodes in contact during an elastic impact simulation. The unidirectional ply behaviour is applied to each ply of the plate model, according to its orientation. Cohesive zone elements are placed at each interface between two plies of different orientations, so that there are 14 interfaces modelled. The numerical problem is composed of 56,880 elements, which means

92,349 degrees of freedom. The computation lasted about 11 days on 4 CPUs of a 2.93 GHz unit. Comparisons are made on the force history, the damage patterns and the estimated projected delaminated area (Figure 5).

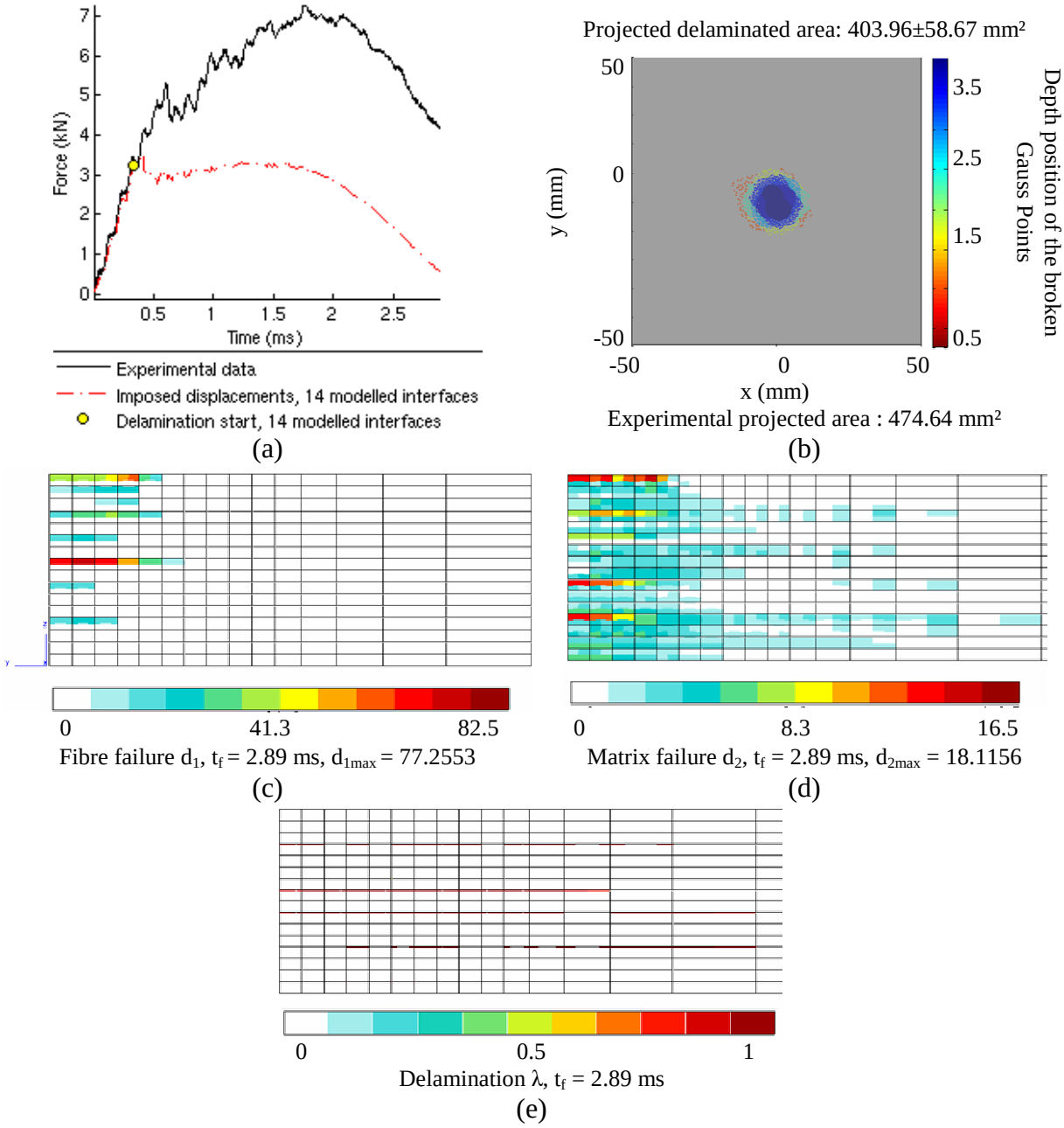

Figure 5. Force history (a), delamination (b, e) and damage (c, d) patterns obtained with the simulation without contact of a quasi-isotropic laminate impacted at 10 Joules.

The use of the cohesive zone models at all interfaces in the numerical model is the only way to capture the first drop in the force history. The computation suggests that this drop occurs shortly after the first delamination. However, the model does not show the rise of the force after this sudden drop. This may be due to the imposed displacements that do not take into account a decrease of the plate stiffness, which could be done with a contact algorithm. The delamination pattern seems to agree quite well with the one observed after the impact testing. The interfaces delaminating in the computation seem to be in good agreement with the interfaces delaminated on the micrograph. The matrix damage pattern has the classical pine

tree shape observed on impacted specimens. Fibre failures are detected by the model just beyond the impactor. Those failures do not appear on the micrographs. The unidirectional ply behaviour law is currently being improved to take into account the absence of failure in hydrostatic loadings. The coupling between intralaminar and interlaminar damage is actually being identified for the unidirectional ply behaviour.

6 Conclusions

An impact damage prediction tool is currently elaborated for laminates. It is based on the unidirectional ply behaviour models developed at Onera and on cohesive zone models. In order to validate these behaviour models for impact cases, tests have been performed on a new drop-weight device. Simplified numerical simulation of the test conditions have been performed for further comparisons of the damage pattern, especially delamination. The numerical damage pattern is in good agreement with the experimental one. This result is currently being validated for other impact test cases, such as simply supported impacted plates, and for other stacking sequences of the impacted specimen. Numerical difficulties, due to the high non linearities of the impact modelling, have to be overcome through explicit dynamic algorithms, such as in *Abaqus/Explicit*.
Once the impact damage prediction tool is fully available, it could be used to study scale effects and damage tolerance in impact cases.

References

[1] Cantwell W.J., Morton J. The impact resistance of composite materials – A review. *Composites*, **22**, pp. 347-362 (1991).
[2] Richardson M.O.W., Wisheart M.J. Review of low-velocity impact properties of composite materials. *Composites: Part A*, **27**, pp. 1123-1131 (1996).
[3] Abrate, S. *Impact on composite structures*. Cambridge University Press, New York (1998).
[4] Laurin F., Carrère N., Maire J.-F. A multiscale progressive failure approach for composite laminates based on thermodynamical viscoelastic and damage models. *Composites: Part A*, **38**, pp. 198-209 (2007).
[5] Huchette, C. *On the complementarity of experimental and numerical approaches for the modelling of damage mechanisms of composite laminates*. PhD thesis of the University of Paris 6 (2005).
[6] Charrier J.-S., Carrère N., Laurin F., Bretheau T., Goncalves-Novo E., Mahdi S. *Proposition of 3D progressive failure approach and validation on tests cases* in "Proceedings of *14th European Conference on Composite Materials*", Budapest, Hungary (2010).
[7] Benziane D.M., Chiaruttini V., Garaud J.D., Feyel F., Foerch R., Osipov N., Quillici S., Rannou J., Roos A., Ryckelynck D. *Z-set/ZeBuLoN: a software suite for mechanics of materials and structural calculations* in "Proceedings of *10th National Symposium on Structural Calculations*", Giens, France (2011).
[8] Alfano G., Crisfield M.A. Finite element interface models for the delamination analysis of laminated composites: mechanical and computational issues, *International Journal of Numerical Methods Engineering*, **50**, pp. 1701-1736 (2001).
[9] ASTM D 7136 / D 7136M. *Standard test method for measuring the damage resistance of a fiber-reinforced polymer matrix composite to a drop-weight impact event* (2007).
[10] Wronsky M. *Coupling of contact and friction with non linear solid mechanics under high deformations. Application to the study of polyurethane foam blocks*. PhD thesis of the University of Technology of Compiègne (1994).